NJC

Accepted Manuscript

This is an *Accepted Manuscript*, which has been through the Royal Society of Chemistry peer review process and has been accepted for publication.

Accepted Manuscripts are published online shortly after acceptance, before technical editing, formatting and proof reading. Using this free service, authors can make their results available to the community, in citable form, before we publish the edited article. We will replace this *Accepted Manuscript* with the edited and formatted *Advance Article* as soon as it is available.

You can find more information about *Accepted Manuscripts* in the Information for Authors.

Please note that technical editing may introduce minor changes to the text and/or graphics, which may alter content. The journal's standard Terms & Conditions and the Ethical guidelines still apply. In no event shall the Royal Society of Chemistry be held responsible for any errors or omissions in this *Accepted Manuscript* or any consequences arising from the use of any information it contains.

ROYAL SOCIETY OF CHEMISTRY

www.rsc.org/njc

Cite this: DOI: 10.1039/c0xx00000x

www.rsc.org/xxxxxx

ARTICLE TYPE

Facile synthesis of spinous-like Au nanostructures for unique localized surface plasmon resonance and surface-enhanced raman scattering

Yan Zhang[a], Bingyu Wang[a], Lidong Li[a]* , Shihe Yang[b], and Lin Guo[a]*

Received (in XXX, XXX) Xth XXXXXXXXX 20XX, Accepted Xth XXXXXXXXX 20XX
DOI: 10.1039/b000000x

By changing the ratios of two cationic surfactants cetyltrimethylammonium bromide (CTAB) and cetyltrimethylammonium chloride (CTAC), irregular quasi-spherical AuNPs, popcorn shaped AuNPs, ricepaper pith shaped AuNPs and the spinous-like Au nanostructures were synthesized via a convenient seed mediated method. The composition of the as-prepared uniform Au nanostructure was characterized by the scanning electron microscopy (SEM), transmission electron microscopy (TEM) and X-ray diffraction (XRD). The morphological evolution and kinetics mechanism were well explained by morphological changes at different ratios of surfactants. Systematical analysis revealed that the generation of Au nanostructures with different degrees of tips and the morphology evolution strongly depended on the controlling of the two surfactants ratios, which further effect their localized surface plasmon resonance (LSPR) properties in both visible and near-infrared regions. Moreover, the spinous-like Au nanostructures showed obvious surface-enhanced Raman scattering activity for crystal violet (CV) dye, which implied that the irregular quasi-spherical AuNPs, popcorn shaped AuNPs, ricepaper pith shaped AuNPs and the spinous-like Au nanostructures could be used in applications such as electronics, catalysis, and imaging.

1. Introduction

Gold nanostructures have drawn significant attention, because of their unique properties such as the optical properties, which are of great importance for the applications in the fields of photonics, electronics, sensing, and other various biomedical uses.[1] Because the particular properties of the gold nanostructures are largely dependent on their shapes and sizes, nowadays, large numbers of literatures were reported for obtaining gold nanostructures with controlled shapes and sizes. For example, through altering the feed ratio of hydroquinone, seeds, and additional $HAuCl_4$, Jing Li developed an aqueous synthesis method to control the morphologies and sizes of urchin-like gold nanoparticles (NPs).[2] By simply adding a small amount of CTAB, Luis M. Liz-Marzán group reported the gold nanostars could easily undergo reshaping into spherical particles.[3] Luis M. Liz-Marzán demonstrated that CTAC can be used to induce the seedless formation of highly anisotropic, twisted single crystalline Au nanoparticles in a single step.[4] Lansun Zheng group developed concave Palladium nanocubes with high-index surfaces using CTAC and CTAB.[5] Considering the methods mentioned above, surfactants are often used in the process of preparation, as we know that surfactants can induce the preferential growth along some specific directions to obtain the specific morphology. Though scholars have done some work by using CTAB or CTAC to synthesize several types of morphologies, the spinous-like gold nanostructures controlled by CTAC and CTAB have rarely been reported.

Herein, the as-prepared spinous Au nanoparticles with the central core and the tips can be dedicatedly modulated by the different ratios of surfactants CTAC and CTAB. As we know, the cationic surfactant CTAB and CTAC have been widely used as stabilizer in colloidal dispersions of AuNPs with various morphologies. It's reported that the CTAB is essential to preferentially etch the highly curved tips[3], and the CTAC leads to the generation of nanoparticles with stellated features.[6-8] Therefore, in our system, the interaction between two surfactants helps to form irregular quasi-spherical AuNPs, popcorn shaped AuNPs, ricepaper pith shaped AuNPs and the spinous-like Au nanostructures, which present unusual LSPR properties.

As we know，UV-visible to near-infrared NIR spectroscopy can provide crucial information about the electronic properties of

nanoparticles and optical properties of anisotropic nanostructures, which are significantly different from those of the isotropic nanostructures, in spite of identical sizes.[9] Surface plasmon resonance (SPR) bands extended from UV-visible NIR region are very dependent on the size, shape, and particulate interactions of gold nanostructures. As the size increased or multiple bands of anisotropic appeared, the SPR band will red shift to a longer wavelength.[10] Because the increasing interest of using various synthetic methods offers a process to tightly control the particle size and shape, P Senthil Kumar et al synthesized nanostars with single crystalline tips in the presence of preformed Au nanoparticle seeds.[1] Minghua Liu group developed a vesicle-directed generation method to gold nanoflowers with obvious surface-enhanced Raman scattering activity.[10] Ravi K. Biroju and P. K. Giri had demonstrated effcient physical functionalization of single layer graphene with Au nanoparticles mediated by in-plane defects in graphene grown by a chemical vapor deposition technique. The effect of an ultrathin Au layer on the single layer, bi layer, and few layer graphene with intrinsic defects was studied by resonance Raman spectroscopy and high resolution transmission electron microscopy (HRTEM).[11] Besides, the as-prepared spinous structure has the excellent properties, such as, surface-enhanced Raman scattering activity for crystal violet (CV) dye. The reason can be attributed to that more tips and edges of spinous shape which contribute to the larger specific surface area, provide more active SERS sites and improve the intensity of SERS properties. The enhance factor for CV can reach 10^7, which was rarely reported.[12-14]

In this article, a simple strategy for synthesizing Au spinous-like nanoparticles with sharp edges and tips was described, and two surface plasmon resonance absorption modes were presented. This special nanostructure shows a very high sensitivity to local changes in the dielectric environment, as well as greater enhancement of the electricmagnetic field around the nanoparticles, which constitute the basis of localized surface plasmon resonance (LSPR) or excellent surface enhanced Raman scattering (SERS) analyses. The morphological evolution and kinetics mechanism were well explained by the morphological changes at different ratios of surfactants. Furthermore, this unique morphology exhibits a great potential for future catalysis and biosensing applications.

2. Experimental Section

Hydrochloroauric acid tetrahydrate ($HAuCl_4.3H_2O$) were purchased from Alfa Aesar, sodium borohydride ($NaBH_4$) was obtained from Guangdong Guanghua Chemical Factory Co., Ltd, cetyltrimethylammonium bromide (CTAB) from Tianjin Fine Chemical Industry Research Institute and cetyltrimethylammonium chloride (CTAC) from Tianjin Jingke Fine Chemical Industry Research Institute were used as protecting agents, ascorbic acid (AA) form Beijing Boaoxing Biological Technology Limited Liability Company were used as reducing, ammonia water and crystal violet (CV，MW407.99) were supplied by Beijing chemical works and Tianjin Jingke Fine Chemical Industry Research Institute, respectively.

CTAC-capped Au seed solution was prepared by injecting $NaBH_4$ solution into a mixture of CTAC and $HAuCl_4$. 100 uL seed solution was added in the growth solution containing ammonia water (0.1M, 50 mL), $HAuCl_4$ (1×10^{-2} M, 500 μL), and ascorbic acid (0.1 M, 100 μL). The influence of different ratios of CTAC to CTAB on the reshaping process was studied by varying their volumes as follows: CTAC (0.1 M, 8 mL), CTAB (0.1 M, 2 mL); CTAC (0.1M, 6 mL), CTAB (0.1 M, 4 mL); CTAC (0.1 M, 4 mL), CTAB (0.1 M, 6 mL); CTAC (0.1 M, 2 mL), CTAB (0.1 M, 8 mL), to obtain from irregular quasi-spherical AuNPs to almost complete spinous shape AuNPs. This solution was put in a 30 ℃ water bath overnight. The as-prepared AuNPs were washed three times by centrifugation (10000 rpm, 10 min).

The SERS substrate was prepared by dropping the above-prepared sample of 10 μL onto a carefully cleaned silicon plate, which was allowed to dry naturally in air. The substrate was immersed into 1×10^{-7} mol L^{-1} crystal violet (CV) water solution for 30 min. After drying at room temperature, it was then rinsed with deionized water and absolute ethanol several times to remove the free CV molecules.

Scanning electron microscopy (SEM) images were carried out with a Hitachi S-4800. High-resolution transmission electron microscopy (HRTEM) images were obtained using a JEOL JEM-2100F microscope. The UV-Vis spectrum was preceded in the spectrophotometer (UV-3600, Shimadzu). Raman spectra were recorded on a Jobin Yvon (JY HR800) spectrometer employing a 633-nm laser line as the excitation source. The Raman band of a silicon wafer at 520 cm^{-1} was used to calibrate the spectrometer. The spectra were obtained by using a 50× objective lens to focus the laser beam onto a spot with ~1.9 μm^2.

3. Results and Discussion

In this article, the four different kinds of Au nanostructure (from irregular quasi-spherical AuNPs to almost complete spinous shape AuNPs) were prepared by varying the volume ratios of CTAC to CTAB. **Figure 1** shows typical SEM and TEM images of synthesized the spinous-like gold nanostructures. From the SEM images in **figure 1 (b)**, it can be found that individual nanostructure consists of inhomogeneous distributed multiple pricks (tips). **Figure1 (a)** manifests the overall uniformity in shape and size of these nanostructures. In order to examine the detailed structure of the as-synthesized nanostructures, high resolution transmission electron micrographs (HRTEM) were recorded in **figure 1 (c)**, **(d)**, **(e)** and **(d)**. **Figure 1 (c)** shows that the nanostructures are uniform in shape and size with branch structures. A representative TEM image of such a nanostructure is shown in **Figure 1(d)**. The magnified view of the red frame region in **Figure 1(e)** is shown in **Figure 1 (f)**. Multiple tips are clearly seen from the TEM image with the shape resembling to that of a spinous-shaped nanostructure.[3] Additional crystallographic information can be obtained from the atomic lattice fringes. The lattice fringe spacing on one of the tips was determined to be ~0.24 nm, corresponding to the interplanetary distance of (111) plane for the face centered cubic (fcc) gold. Through the **figure 1**, the maximum length of such a nanostructure along the longest tip is measured to be 300 ~400 nm and a single tip was considered to protrude from the body center, with the diameter and length measured for one of the tips ~60 and ~110 nm, respectively.

The obvious variation of AuNPs morphology by altering the ratios of CTAC to CTAB clearly reveals the reshaping process (**figure 2(a-d)**). With increasing the ratios of CTAC to CTAB from 1:4, 2:3, 3:2 to 4:1, the apparent surfaces of AuNPs gradually changed from irregular quasi-spherical AuNPs, popcorn shaped AuNPs, ricepaper pith shaped AuNPs, to almost completely spinous shaped AuNPs. As shown in the SEM images of **figure 2**, the central core of Au nanostructure was gradually surrounded by bumped structures which become longer and thinner with the increasing ratio. This process is demonstrated by the mechanism model in **figure 2 (e)**. This shape evolution can be confirmed by the UV-Vis-NIR spectra during the CTAC and CTAB-induced reshaping process. **Figure 2 (f)** shows the UV-Vis-NIR spectra for the dispersion of gold nanostructures in ethanol, revealing a size and/or morphology variation of tips and NPs, while the unexpected surface plasmon resonance absorption peaks appear at shorter wavelength region, although very low intensity, which is due to the presence of large number of nanometer sized tips with variable lengths and diameters. It is a common phenomena that a broad absorption occurs in the near-infrared region for larger sized anisotropic gold nanostructures.[9,15] Accordingly, the surface plasmon resonance absorption peak of as-prepared NPs shift from the 615 nm to the weaker shoulder around 847 nm (**Figure 2f**), and the SPR band is broadened and moves to longer wavelength, then beyond the visible region, all of which are typical for NP with increasing diameters. Meanwhile, continuous blue-shift from 455 nm to 415 nm is also observed, which is in good agreement with the results for longer and thinner morphological changes.

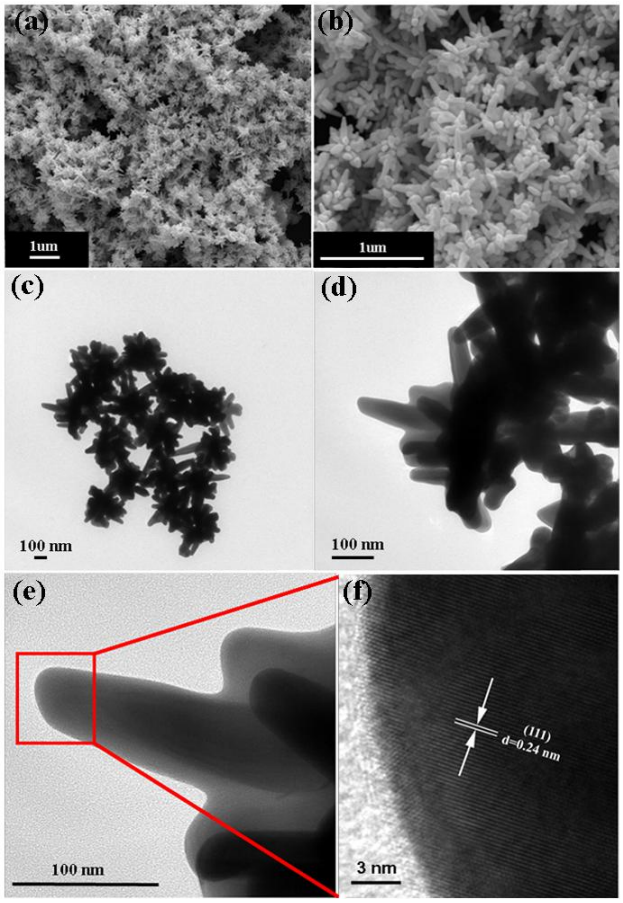

Figure 1. (a,b) Low and high magnification SEM image of the spinous-like AuNPs, (c) TEM image of the spinous shape AuNPs, (d) TEM image of a single spinous-like AuNPs, (e) partial magnified TEM image of the spinous-like AuNPs, (f) HRTEM image of the spinous-like AuNPs.

In our experiment, it can be suggested that the morphology of AuNPs is mainly influenced by increasing the ratios of CTAC to CTAB. As reported before, both CTAB and CTAC can be used to synthesize nanostructures. CTAC mainly attributed to

the generation of nanostructures with stellated features.[6-8] Whereas, CTAB is essential to preferentially etch the highly curved tips.[3] When the two surfactants were added into the system, the coordination affinity of Br^-–CTA^+ to gold was stronger than Cl^-–CTA^+, which allows CTAB adsorption on the tips, leading to etching of weakly bound Au atoms from the sharp convex zones at tip ends.[3] So as the percentage of CTAC to CTAB increases, bumped particles are initially formed until the longer and thinner pricks appear, the uniform spinous-like shaped AuNPs are formed finally. Of note, simply adding CTAB often results in the uneven smooth surfaces of Au nanoparticles or the adding of CTAC alone often leads to the irregular spinous Au nanoparticles as shown in figure S5.

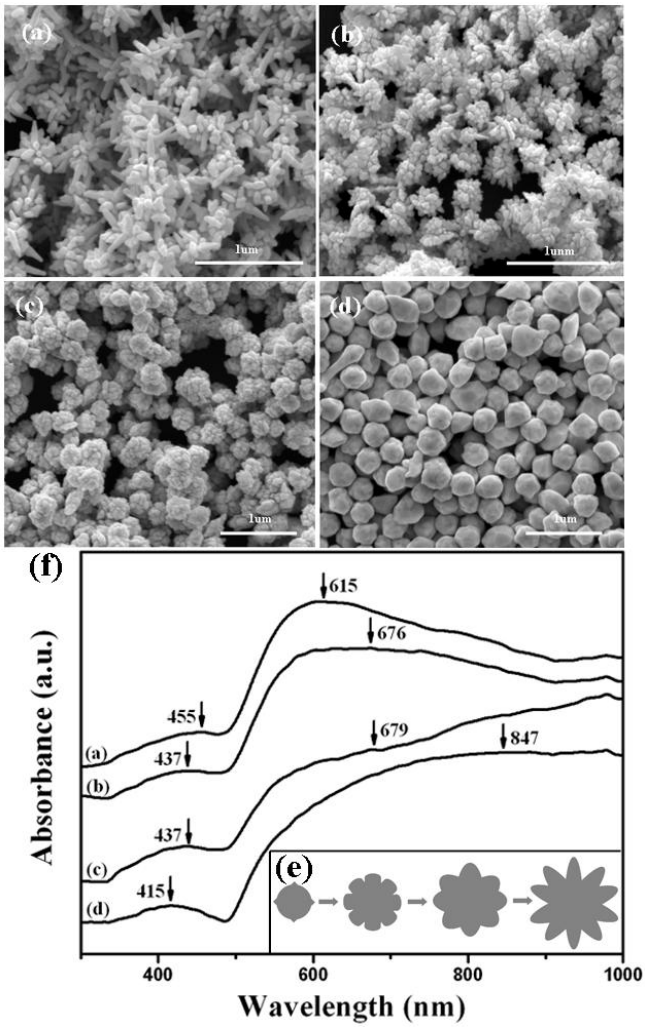

Figure 2. SEM images and UV-vis spectra of gold nanostructures obtained with a varying ratios of CTAC to CTAB: (a) 1:4; (b) 2:3; (c) 3:2; (d) 4:1. (e) Schematic illustration for changing process from irregular approximate spherical to spinous shape AuNPs. (f) The UV-vis spectra of gold nanostructures obtained with a varying ratios of CTAC to CTAB.

As shown in figure 3, all peaks can be well indexed to the {111}, {200}, {220}, {311} and {222} planes for a face-centered cubic lattice (JCPDS card no.65-2870) of Au. No impurity phases are detected, indicating the formation of pure and highly crystallized Au.

Under the different PH of solutions, the morphology of gold nanostructures were characterized by the SEM as shown in figure 4 and 5. With the acid additive, as the ratios of CTAC and CTAB increased, the bumped structures, which grown out from the central core of Au nanostructure, gradually become longer and thinner. The same phenomenon was also existed in the environment with neutral additive NaBr. So the changing rule of morphology was the same as the situation with the alkalinity additive ammonia water.

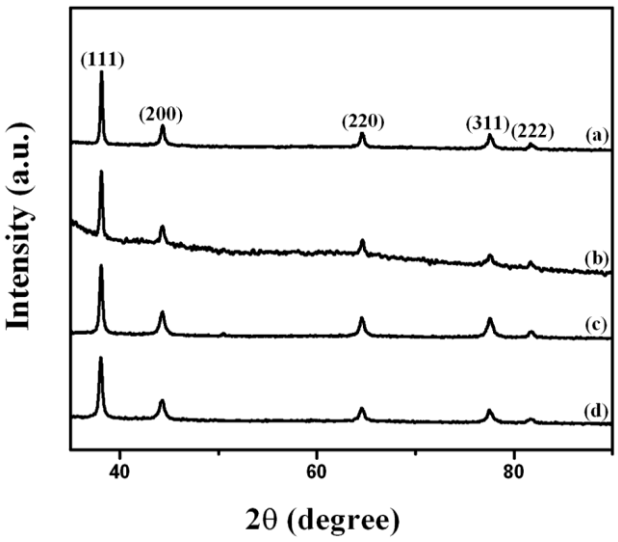

Figure 3. XRD patterns of Au nanostructures by different ratios of CTAC to CTAB: (a) 1:4; (b)2:3; (c) 3:2; (d) 4:1.

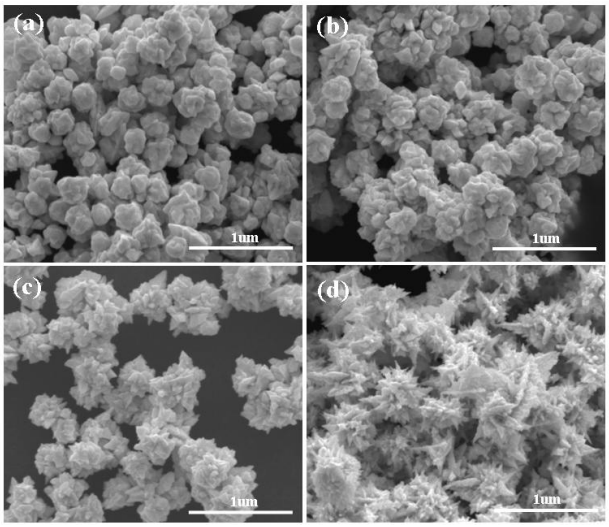

Figure 4. SEM of Au nanostructures in the presence of HCl (1.0M, 200ul) and $AgNO_3$ (0.01M, 40ul) by different ratios of CTAC to CTAB: (a) 1:4; (b) 2:3; (c) 3:2; (d) 4:1.

Some other control experiments were performed in figure

S1 to S6. From figure S1 to S4, changing the volume of silver nitrate solution while keep the other experiment parameters unchanged, the results show the same regular that with the ratios of CTAC and CTAB increased, the bumped structures, which grown out from the central core of Au nanostructure, gradually become longer and thinner. Keep the ratios of CTAC and CTAB unchanged, with the increasing of the volume of silver nitrate, the bumped structures of nanostructure were increased. From the figure S5, with the same PH of the solution, we can see that nanostructure gold with the only surfactant CTAC is exhibited more spinous structures than the nanogold with the only surfactant CTAB. In figure S6, spiny convex of gold nanoparticles were decreased when CTAC was changed to DDAB, while keeping the ratio of the two surfactants unchanged. So the experiment condition which is discussed in the main text is the most proper and optimized condition to prepare the different tips of gold nanostructures.

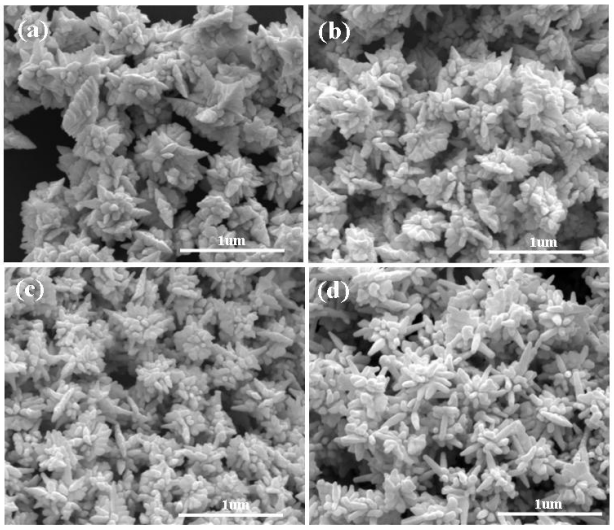

Figure 5. SEM of Au nanostructures in the presence of NaBr (0.1M, 50ul) by different ratios of CTAC to CTAB: (a) 1:4; (b) 2:3; (c) 3:2; (d) 4:1.

Surface-enhanced Raman scattering (SERS) is a powerful tool for optical detection and for spectroscopic investigation of single molecules absorbed on certain metallic substrates, which were composed by well-defined nanostructured materials. To investigate the SERS sensitivity of the Au nanostructures synthesized by using different ratios of CTAC to CTAB, Raman spectra of 1.0×10^{-7} M crystal violet (CV) adsorbed on the surface of Au NPs were measured. The SERS response was examined by using crystal violet (CV) dye as the probe molecule, due to its distinct Raman features and its ability to form a self-assembled monolayer or sub-monolayer on Au nanostructures without any further chemical modification.[16-18] The SERS spectra of CV adsorbed on the irregular quasi-spherical AuNPs, popcorn shaped AuNPs, ricepaper pith shaped AuNPs and the spinous-like Au nanostructures, excited with the 633 nm laser line are presented in **figure 6**.

The as-prepared Au nanostructure synthesized by 4:1 ratio of CTAC to CTAB shows the highest SERS activity as shown in **figure 6d**, while the CV molecules on the Au nanostructure with 3:2 ratio of CTAC to CTAB generates weaker Raman signals (figure 6c) when excited under the same conditions. And the SERS intensity of Au nanostructures modified by 2:3 ratio of CTAC to CTAB in **figure 6b** also exhibits greater enhancement than the Au in **figure 6a**, but less than Au nanostructures in **figure 6d** and **6c**. As we know, the branches and tips of gold nanomaterials, which were the reason for the formation of sharp peaks and valleys, can drastically increase the ratio of total surface to volume. The tips are potential "hot spots" for localized near-field enhancements[19] and could potentially enhance the Raman scattering on the highly branched gold nanostructures. As a result, the uneven nano-tips presented in the rougher Au NPs surface facilitate to provide greater enhancement on SERS signals than the nanostructure with smooth surface. These results confirm that the Au nanostructures with the CTAC and CTAB ratio of 4:1 indeed exhibit an excellent capability to enhance Raman signals of molecules adsorbed on their surfaces and show the great sensitivity of SERS, thus it could be used as an ideal active SERS substrate. With regard to the position of the peaks for CV probe molecule, specific assignments are shown in Table 1.

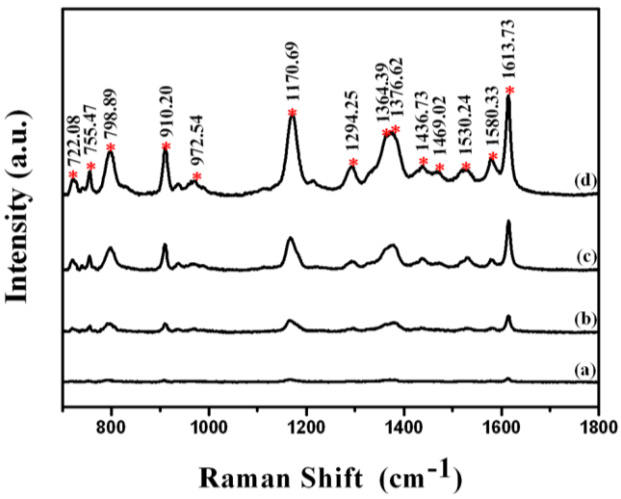

Figure 6. SERS spectra of crystal violet absorbed on the different Au nanostructures synthesized by using different ratios of CTAC to CTAB: (a) 1:4; (b) 2:3; (c) 3:2; (d) 4:1. All of the spectra were recorded as the results of 10 s accumulation.

Enhancement Factors

It is generally considered that the enhancement of a1 mode in SERS mainly originated from EM mechanism. To evaluate the enhancement activity more quantitatively, two predominant a1 bands discussed earlier in the paper were selected to determine the enhancement factor (EF) according to the following equation:[19,20]

$$EF= \frac{I_{SERS}/N_{ads}}{I_{bulk}/N_{bulk}} \quad (1)$$

Where, I_{SERS} and I_{bulk} are the measured vibration intensity in the SERS and normal Raman spectra, respectively. N_{bulk} and N_{ads} are the molecule number of solid and adsorbed CV in the laser illumination volume, respectively. And N_{bulk} was acquired via eq 2:

$$N_{bulk}=Ahn_{bulk}=Ah\frac{\rho_{bulk}}{M_{bulk}}N_A \quad (2)$$

The illuminated volume was calculated as the product of the area of the laser spot A (~1.9 μm^2) and the penetration depth h of the focused laser (~15.4 μm). Considering the density (1.089 g/cm^{-3}) of bulk CV, N_{bulk} was calculated as 4.7×10^{10}. As for SERS samples, N_{SERS} could be obtained via eq 3:

$$N_{SERS}= \frac{AN_{sub}A_{sub}}{\sigma} \quad (3)$$

A is the area of the focal laser spot (~1.9 μm^2). Asub is the occupied area of individual nanoparticle (~0.12 μm^2) andσ represents the surface area occupied by one adsorbed CV molecule about 4.35 nm^2 according to the result of our estimate in the supporting information. Assuming that a layer of Au nanoparticles deposited on the substrate homogeneously, number density of AuNPs (Nsub) could be counted from the SEM figure.

By substituting the values of the variables into eq 1, enhancement factor (EF) of CV adsorbed on spinous-like AuNPs, ricepaper pith shaped AuNPs, popcorn shaped AuNPs and irregular quasi-spherical AuNPs were estimated to be about 1.7×10^7 , 1.3×10^7, 3.1×10^6 and 7.5×10^5. Through the analysis of the results, an enhancement factor of 10^5~10^7 that was mainly contributed by electromagnetic mechanism was finally estimated.

4. Conclusion

In summary, irregular quasi-spherical Au nanoparticles, popcorn shaped Au nanoparticles, ricepaper pith shaped Au nanoparticles, and spinous-like Au nanoparticles have been synthesized by modulating the ratios of different surfactants CTAC and CTAB using seed mediated method. The Scanning electron microscopy (SEM), transmission electron microscopy (TEM) and X-ray diffraction (XRD) were used to characterize the morphologies of the as-prepared uniform Au nanostructures. Due to the changing core and tips sizes of the Au nanostructures, the exceptional optical properties of localized surface plasmon resonance (LSPR) in both visible and near-infrared regions were investigated. The effect of CTAC and CTAB on morphological changes was also discussed in our work, the morphological evolution and kinetics mechanism were well explained by the simulation mode which finely matched with the morphological results. The excellent surface-enhanced Raman scattering of the spinous-like Au nanostructures was demonstrated to be active for detecting crystal violet (CV) dye. These implied that the irregular quasi-spherical Au nanoparticles, popcorn shaped Au nanoparticles, ricepaper pith shaped Au nanoparticles, and the spinous-like Au nanoparticles are promising nanomaterials for promoting the technical applications in electronics, catalysis, and imaging.

Table 1. Raman frequencies (cm^{-1}) and assignments of the main bands of CV in figure 6

Raman shift (cm^{-1})	band assignment
1613.73 cm^{-1}	υas(C=C) ring
1580.33 cm^{-1}	υs(C=C) ring
1530.24 cm^{-1}	υas(C-C) ring
1469.02 cm^{-1}	υas(C-C)+δ(ring)
1436.73 cm^{-1}	υs(C-C)+δ(ring)
1364.39, 1376.62 cm^{-1}	υ(N-Phenyl)
1294.25 cm^{-1}	υs(C-C) ring
972.54, 1170.69 cm^{-1}	δ(C-H)
910.20 cm^{-1}	ring skeletal vibration of radical orientation
722.08, 755.47, 798.89 cm^{-1}	γ(C-H)

Acknowledgment. This work was financially supported by the National Basic Research Program of China (2010CB934700), the National Natural Science Foundation of China (21273001, 51272012, 51302208), Fundamental Research Funds for the Central Universities (YWF-14-HHXY-009), and Specialized Research Fund for the Doctoral Program of Higher Education (20111102130006).

[a] *School of Chemistry and Environment, Beihang University, Beijing 100191, PR China. lilidong@buaa.edu.cn, guolin@buaa.edu.cn*
[b]*Department of Chemistry, Hong Kong University of Science and Tecnology, Kowloon, Hong Kong*

† Electronic Supplementary Information (ESI) available: details of any supplementary information available should be included here. See DOI: 10.1039/b000000x/

References

1. Pandian Senthil Kumar, Isabel Pastoriza-Santos, Benito Rodr íguez-Gonz´alez, F Javier Garc´ıa de Abajo and Luis M Liz-Marz´an, *Nanotechnology*, 2008, **19**, 015606.
2. Jing Li, Jie Wu, Xue Zhang, Yi Liu, Ding Zhou, Haizhu Sun, Hao Zhang, and Bai Yang, *J. Phys. Chem. C*, 2011, **115**, 3630-3637.
3. Laura Rodríguez-Lorenzo, JoséM. Romo-Herrera, Jorge Pérez-Juste, Ramón A. Alvarez-Puebla, Luis M. Liz-Marzán, *J. Mater. Chem.*, 2011, **21**, 11544-11549.
4. Paula C. Angelomé, Hamed Heidari Mezerji, Bart Goris,‡ Isabel Pastoriza-Santos, Jorge Pérez-Juste, Sara Bals, and Luis M. Liz-Marzán, *Chem. Mater.*, 2012, **24**, 1393-1399.
5. Jiawei Zhang, Lei Zhang, Shuifen Xie, Qin Kuang, Xiguang Han, Zhaoxiong Xie, and Lansun Zheng ,*Chem. Eur. J.*, 2011, **17**, 9915-9919.
6. Ma, Y. Y., Kuang, Q., Jiang, Z. Y., Xie, Z. X., Huang, R. B., Zheng, L. S., *Angew. Chem. Int. Ed.*, 2008, **47**, 8901-8904.
7. Wu H. L., Chen C. H., Huang M. H., *Chem. Mater.*, 2009, **21**, 110-114.
8. Jian Zhang, Mark R. Langille, Michelle L. Personick, Ke Zhang, Shuyou Li, Chad A. Mirkin, *J. AM. CHEM. SOC.*, 2010, **132**, 14012-14014.
9. Jadab Sharma, Yian Tai, and Toyoko Imae Talanta, *J. Phys. Chem. C*, 2008, **112**, 17033-17037.
10. Ling Zhong, Xiaodong Zhai, Xuefeng Zhu, Pingping Yao, and Minghua Liu, *Langmuir*, 2010, **26**, 5876-5881.
11. Ravi K. Biroju and P. K. Giri, *J. Phys. Chem. C*, 2014, **118**, 13833−13843.
12. Osman M. Bakr, Benjamin H. Wunsch, and Francesco Stellacci, *Chem. Mater.*, 2006, **18**, 3297-3301.
13. S.Y. Li, M. Wang, *IET Nanobiotechnol.*, 2012, **6**, 136–143.
14. Ju-Hyun Kim, Taejoon Kang, Seung Min Yoo, Sang Yup Lee, Bongsoo Kim and Yang-Kyu Choi, *Nanotechnology*, 2009, **20**, 235302.
15. (a) Sharma, J., Vijayamohanan, K. P. J., *Colloid Interface Sci.*,2006, **298**, 679-684. (b) Jena, B. K., Raj, C. R., *Chem. Mater.*, 2008, **20**, 3546-3548.
16. Lin-Fei Zhang, Sheng-Liang Zhong, An-Wu Xu, *Angew. Chem.*, 2013, **125**, 673-677.
17. (a) B. Lim, M. Jiang, P. H. C. Camargo, E. C. Cho, J. Tao, X. Lu, Y. Zhu, Y. Xia, *Science*, 2009, **324**, 1302-1305; (b) J. Chen, T. Herricks, Y. Xia, *Angew. Chem.*, 2005, **117**, 2645-2648; c) J. Watt, S. Cheong, M. F. Toney, B. Ingham, J.Cookson, P. T. Bishop, R. D. Tilley, *ACS Nano*, 2010, **4**, 396-402; d) J. X. Fang, S. Y. Du, S. Lebedkin, Z. Y. Li, R. Kruk, M. Kappes, H. Hahn, *Nano Lett.*, 2010, **10**, 5006-5013; e) M. J. Mulvihill, X. Y. Ling, J. Henzie, P. D. Yang, *J. Am. Chem. Soc.* , 2010, **132**, 268-274.
18. (a) C. Chenal, R. L. Birke, J. R. Lombardi, *ChemPhysChem*, 2008, **9**, 1617-1623; b) K. J. hajehpour, T. Williams, L. Bourgeois, S. Adelojua, *Chem. Commun.*, 2012, **48**, 5349-5351.
19. Jixiang Fang, Shuya Du, Sergei Lebedkin, Zhiyuan Li, Robert Kruk, Manfred Kappes, Horst Hahn, *Nano Lett.* , 2010, **10**, 5006-5013.
20. Y. L. Wang, X. Q. Zou, W. Ren, W. D. Wang, E. K. Wang, *J. Phys. Chem. C*, 2007, **111**, 3259-3265.